Chapter 6: Comparative Studies of Bulk Processed Complex Al-Si Alloys

6.1 Introduction

This chapter presents comparative study of the deformation behavior of the complex Al-Si alloys such as Al-18Si-2.5Cu-0.6Fe (Alloy A), Al-11Si-2.5Cu-0.6Fe (Alloy B) and Al-7.4Si-2.5Cu-0.6Fe (Alloy C) during bulk processing and its effect on the tribo-mechanical characteristics of the forged alloys. The Al-Si alloys were cast by varying the Si wt.% from 18 to 7.4 and, developed three different such complex Al-Si alloys. The bulk processing was performed through different forging operations namely open-die, impression-die and converging die forging. Various process parameters such as reduction rate, working temperature, forming speed, lubrication etc. involved during bulk processing which significantly affect the deformation behavior of the processed alloy. These parameters also affect the microstructural features and engineering properties of the processed alloy. Therefore, careful selection of different processing parameters must be required to achieve the desired bulk processed products with optimum engineering properties of the alloy.

6.2 As-cast morphology and physical properties of the Al-Si alloys

As discussed earlier in the sections 3.2.1, 4.2.1 and 5.2.1, the cast morphology of the Al-Si alloy contains coarse primary and needle-shaped eutectic Si particles along with complex intermetallic compounds non-uniformly dispersed in the Al matrix. Such morphology formed in the alloy due to non-uniformity in the cooling rate during solidification. The presence of the hard and brittle second phase particles in the Al matrix reduces the engineering properties of the alloy. Table 6.1 shows the microstructural feature and physical properties of the complex as-cast Al-Si alloys. Table 6.1 shows that

UST increased slightly but the hardness of the alloy significantly increased with increase in the Si wt.% in the alloy. It may be due as increased Si wt.% cause more dispersion of the Si particles in the matrix which decreases the volume fraction of soft Al matrix. Therefore, applied load transfer from the soft Al matrix to hard Si particles and, thus increases the hardness of the Al-Si alloy. Due to increase in coarse microstructure as increase the Si wt.%, the UTS of the alloy was increased very slight.

Table 6.1 Microstructural feature and physical properties of the as-cast alloy

Alloys compositions	Si particles (Mean diameter/standard deviation) (μm)		Intermetallic phases	UTS (MPa)	Hardness (HV_{100})
	Primary	Eutectic			
Al-18Si-2.5Cu-0.6Fe (wt.%) Alloy A	41.90/25.80	39.60/15.20	β-$Al_{4.5}FeSi$, and Al_2Cu	115±6	78±3
Al-11Si-2.5Cu-0.6Fe (wt.%) Alloy B	49.30/21.43	23.55/11.30	β-$Al_{4.5}FeSi$, and Al_2Cu	111±4.5	51±3
Al-7.4Si-2.5Cu-0.6Fe (wt.%) Alloy C	-	25.33/15.02	β-$Al_{4.5}FeSi$, and Al_2Cu	110±5	44±4

6.3 Deformation behavior of the complex Al-Si alloys during bulk processing through open die, impression die and converging die forging

The results from sections 3.2.2, 4.2.2 and 5.2.2 show the deformation behavior of the complex hypereutectic Al-18Si-2.5Cu-0.6Fe, eutectic Al-11Si-2.5Cu-0.6Fe, and hypoeutectic Al-7.4Si-2.5Cu-0.6Fe alloys respectively under various forging conditions. The results reveal that open-die forging of Alloy A and B is not feasible and generates severe surface cracks in the preform under both room temperature and 300°C, while microcracks were developed on the surface of Alloy C preform. It may be due to the presence of the coarse primary and eutectic Si particles along with intermetallic phases initiate stress concentration with Al matrix and generate micro cracks which further

developed severe surface cracks as the deformation progressed. Since there was no restriction of outward metal flow in open die condition, therefore severe surface cracks were developed on the surface of the preform of Alloy A and B during forging. The results also depict that the severity of surface cracks was higher in Alloy A as compared to Alloy B. It may be due to higher wt.% of the Si in the Alloy A increases its hardness and brittleness which in turns increase in the severity of the surface cracks. Due to the absence of primary Si particles and low hardness value, few micro-surface cracks were developed on the surface of the of Alloy C preform during open die forging.

In impression die forging of the Alloys A and B at room temperature shows the surface cracks in the preform even though the presence of the die wall restriction. It may be due to ineffective recovery and increased flow stresses, the stress concentration initiates between regions of second phase particles and Al matrix, which further propagate during processing. The Alloy C depicts the impression die forging of the Alloy C was feasible at room temperature and crack-free smooth surface was obtained during processing.

However, the impression die forging of all Alloys A, B and C was feasible at elevated temperatures and defect free products were achieved during processing. It may be due forging of the Al-Si alloy at elevated temperatures induced ductility and thus soften the material. During processing the outward flowing metal encounters the die walls which produce back stresses against radially outward flowing material. Since second phase particles initiate surface cracks on the outer periphery of deformed samples during forging but the previously developed back stresses protect the surface against cracks. Also, the recovery process of the soft outward flowing metal was complete which reduced the surface cracks. Therefore, the impression die forging of Alloy A, B and C was feasible and defect free products were obtained. The results show that due to less friction and more surface movement occurred between die wall and preform led to the better surface finish of the product under lubricated interfacial conditions at lower applied load during

impression forging. The converging die forging of Alloy A, B and C were also feasible at elevated temperatures and crack-free sound products were obtained during processing.

6.4 Microstructural features of forged complex Al-Si alloys

The Tables 3.1-3.3, 4.1-4.3, and 5.1-5.2 show the average Si grain sizes of the forged samples of Alloy A, B and C from earlier section 3.2.3, 4.2.3, and 5.2.3 respectively. The results indicate that microstructural refinement in all the alloy during bulk processing. It may be due precipitation of elemental silicon and intermetallic compounds containing Cu, and Fe giving rise to finer precipitates of Si and the intermetallic compounds during homogenization at the pre-set processing temperature. In addition, several coarse particles undergo high speed of deformation during compressive loading. The hard and brittle silicon-intermetallic particles could not sustain the applied load, got fragmented, and uniformly distributed along with laterally flowing soft aluminum matrix. As a result, microstructural refinement was observed with fine particles of Si and the intermetallics in the forged samples as shown in Figures 3.18-3.21, 4.14-4.17 and 5.14-5.17 in the Alloys A, B, and C, respectively. The degree of fragmentation depends on the stress level applied to the sample, orientation of the particle, and its size.

The results also reveal the Alloys A, B and C forged through the converging die show significant microstructural refinement as compared to impression die compression. It may be attributed to the metal flow through the converging section which deforms severely, thus results in more fracture and fragmentation of brittle second phase particles.

The results show that all alloy forged at 400°C was found to be optimum processing temperature in terms of the distribution and fine size of the second phase particles as well refinement of the grains of the matrix during impression die as well as the converging die forging. The optimum refinement in microstructural features of the all forged alloy was achieved at 1.20 aspect ratio (h/d) in impression die and 2.0 reduction ratio (R) in

converging die forging. Therefore, microstructural refinement depends on the working temperatures, aspect ratios or reduction ratios.

6.5 Mechanical properties of the forged complex Al-Si alloys

Figures 6.1-6.2 and 6.3-6.4 show the ultimate tensile strength (UTS) and Vickers hardness of the Alloys A, B and C forged through impression die and converging die under various processing conditions. The results show that UTS and hardness of the forged alloy in all compositions in Alloys A, B and C were significantly enhanced during forging as compared to the as-cast alloy. It may be due to alteration of coarse microstructural features into refined grains and their uniform dispersion in the Al matrix. Due uniform dispersion of the second phase particles in the Al matrix which results in a considerably strong interfacial bonding developed between these particles and the Al matrix. The Figures 6.1-6.4 indicate that Alloys A, B, and C forged at the aspect ratio (h/d) of 1.20 in impression die and 2.0 reduction ratio (R) in converging die were achieved the optimum UTS and hardness value. It may be due to percentage deformation of the alloy was higher at h/d=1.20 (35%) and R=2.0 (51%) which in turns more refinement in the microstructural features and subsequently enhances the UTS and hardness of the alloys. The UTS and hardness were relatively higher for the samples forged at 400°C as compared to the other working temperatures of 300 and 500°C in all compositions of Al-Si alloy.

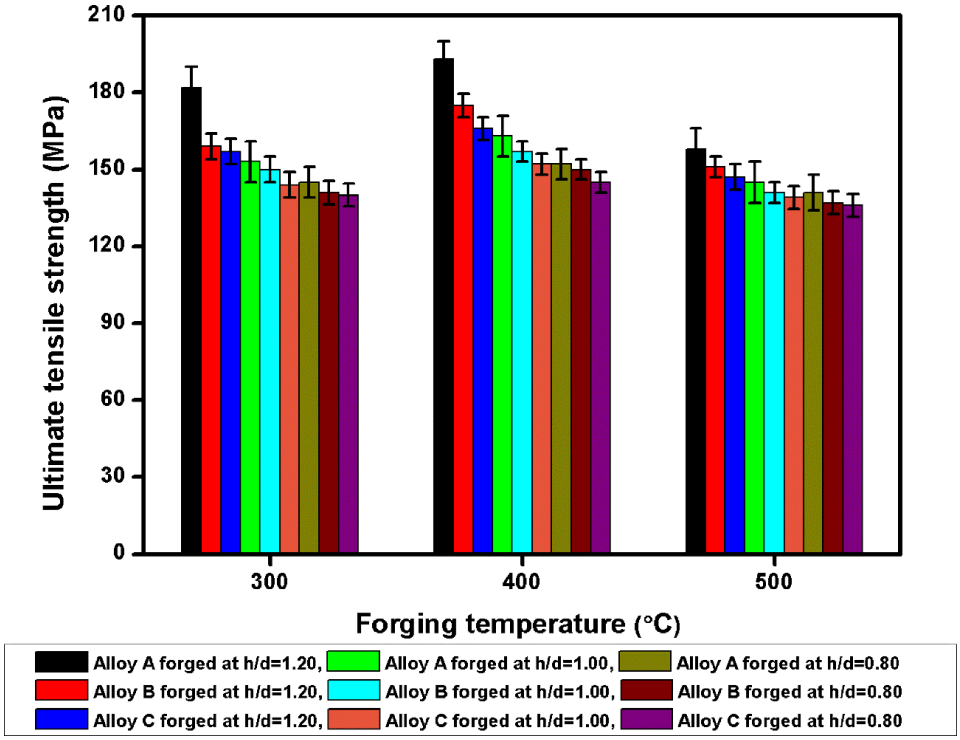

Figure 6.1 Ultimate tensile strength (UTS) of the forged Alloy A, B and C through impression die at different aspect ratios (h/d) and working temperatures (°C)

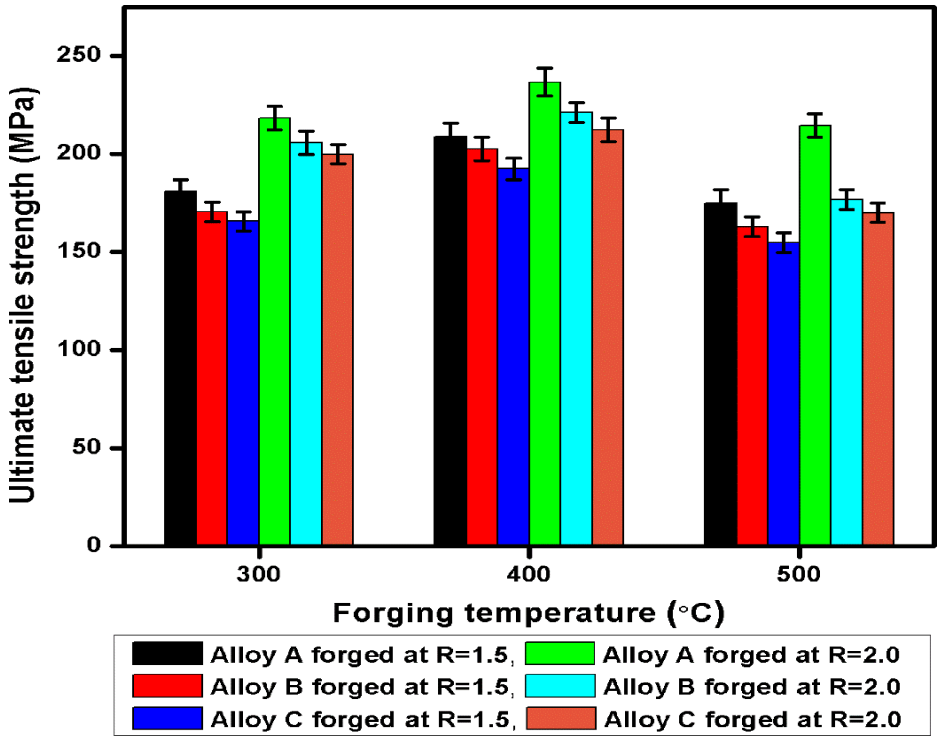

Figure 6.2 Ultimate tensile strength (UTS) of the forged Alloy A, B and C through converging die at different reduction (R) ratios and working temperatures (°C)

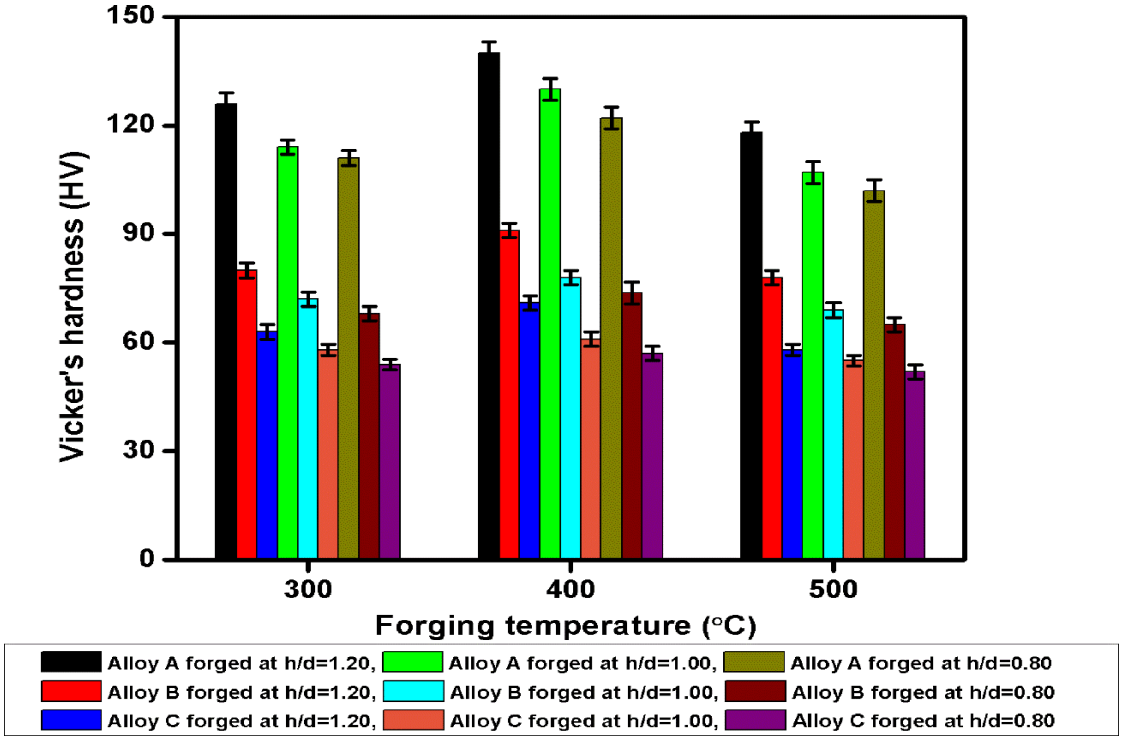

Figure 6.3 Figure 6.2(a) Hardness of the forged Alloy A, B and C through impression die at different aspect ratios (h/d) and working temperatures (°C)

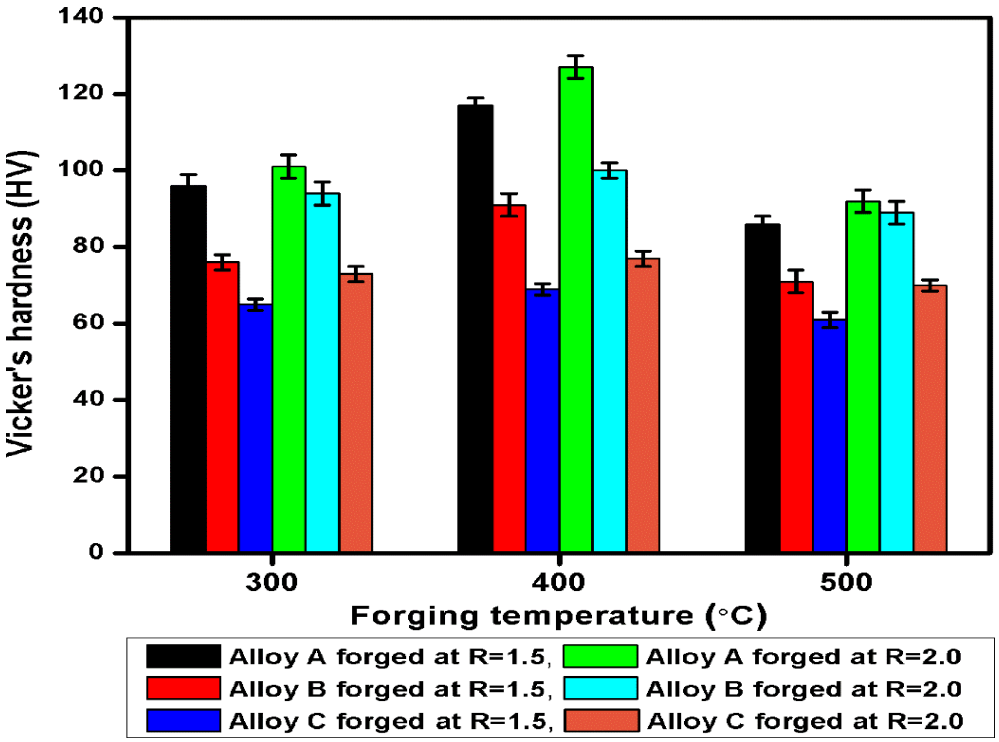

Figure 6.4 Hardness of the forged Alloy A, B and C converging die at different reduction (R) ratios and working temperatures (°C)

6.6 Wear behavior of the complex as-cast and forged Alloys A, B and C

Figures 6.5 and 6.6 show the variation of wear rate with the applied normal load for the as-cast and forged samples of Alloys A, B, and C with reduction ratios R=1.5 and 2.0 respectively. The results reveal that wear resistance of the forged alloys was considerably improved during dry sliding as compared to the as-cast alloy in all processing conditions as shown in Figures 6.5 and 6.6. It may be attributed to refinement in microstructural features and higher hardness the forged alloys. Therefore penetration of the hard counter surface asperity into the forged alloy surfaces was less during dry sliding which in turn reduces the mass loss during dry sliding.

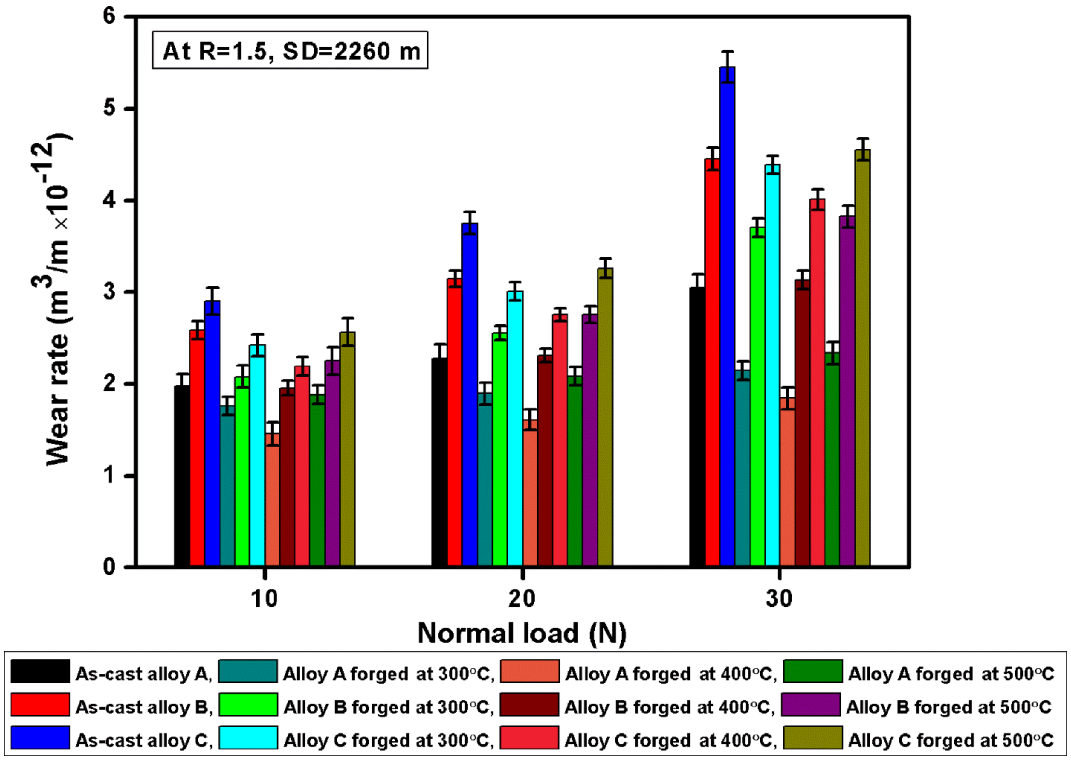

Figure 6.5 Wear rate of the as-cast and forged Alloy A, B and C at R=1.5 and 10, 20, 30 N normal loads

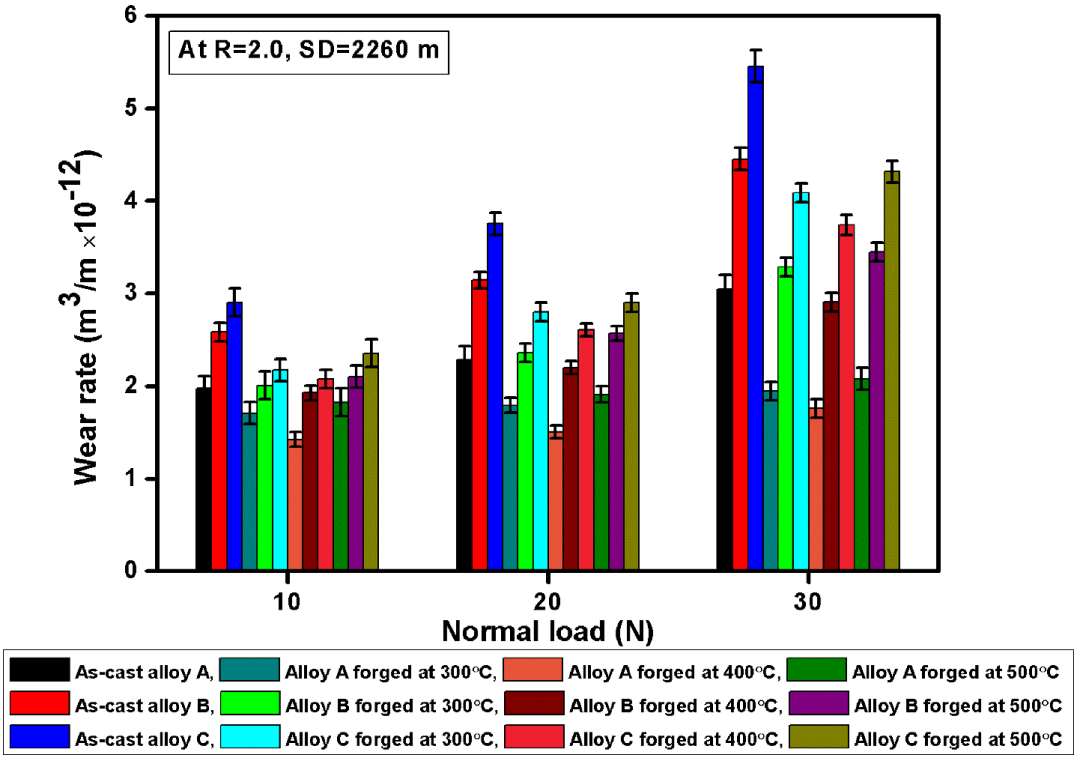

Figure 6.6 Wear rate of the as-cast and forged Alloy A, B and C at R=2.0 and 10, 20, 30 N normal loads

The results also depict that wear resistance of the alloys forged at a reduction ratio (2.0) was slightly higher as compared with 1.5. It was attributed the more hardness value of the forged alloy at reduction ratio 2.0 which enhances the wear resistance of the material. Further, the mass loss was low in all the samples forged at 400°C as compared to the other temperatures 300°C and 500°C. It may be attributed to the less refinement of the microstructure at 300°C which results in the less improvement in the hardness while coarsening occurred at 500°C lowers the hardness which in turn reduces wear resistance of the forged alloys.

6.7 Summary

The important findings of the above chapter are summarized below:

1. The Alloys A and B suffer from the severe surface cracks during open die forging at room temperatures as well as at 300°C and also in impression die forging at room temperature. While Alloy C shows few minute cracks during open die

forging at room temperatures and 300°C. It may be due to the presence of coarse primary Si particles and higher hardness of the Alloys A and B.

2. The defect free products were obtained during impression die forging of the Alloys A, B, and C at elevated temperatures of 300, 400 and 500°C under both lubricating conditions. It may be softening of the alloy at elevated temperature which induced ductility during processing.
3. The microstructural refined occurred in the all forged alloys due to fracture, fragmentation and uniform dispersion of the second phase particles in the matrix during bilk processing.
4. The UTS and hardness of the alloys were significantly improved during forging, it was higher 1.20 aspect ratio and 2.0 reduction at 400°C. The UTS and hardness of the alloy depends on the wt.% of the Si, thus it was higher for the Alloy A having 18 wt.% Si.
5. Wear resistance of the forged alloys was higher as compared with as-cast alloys. It may be due to refined microstructural features and higher hardness of the forged alloys. Due to the higher hardness of the Alloy A shows higher wear resistance as compared to Alloys B and C.

The next chapter 7 presents with complete thesis conclusions and scope for future work.